Preprint Title Factors governing the affinity and selectivity of histone deacetylase inhibitors for the HDAC8 enzyme active site: Implications for anticancer therapy

Authors Nikolay Toshev, Diana Cheshmedzhieva and Todor Dudev

Publication Date 21 Oct 2020

Article Type Full Research Paper

ORCID® iDs Diana Cheshmedzhieva - https://orcid.org/0000-0002-9344-9282;
Todor Dudev - https://orcid.org/0000-0002-8186-2141

Factors governing the affinity and selectivity of histone deacetylase inhibitors for the HDAC8 enzyme active site: Implications for anticancer therapy

Nikolay Toshev[1,2], Diana Cheshmedzhieva[1,*] and Todor Dudev[1,*]

[1]*Faculty of Chemistry and Pharmacy, University of Sofia, 1164 Sofia, Bulgaria*

e-mails: dvalentinova@chem.uni-sofia.bg; t.dudev@chem.uni-sofia.bg

[2]*Plekhanov Russian University of Economics, Stremyanny per. 36, Moscow, 117997, Russia*

Abstract

Disruptions in post-translational modifications of chromatin structure promote uncontrollable cell growth branded as a hallmark of tumor lesions. The overexpression/hyperactivity of histone deacetylases (HDACs) is a common feature for the tumorogenesis and cancer progression. Several inhibitors of histone deacetylases (mainly hydroxamic acid derivatives) have been successfully used as drugs in fighting tumor formations. However, there is no systematic study on the factors controling the affinity and selectivity of this type of inhibitors to the host enzyme thus hampering successful rational design of more potent and selective anticancer drugs. Herein, in an attempt to illuminate the mechanism of the host – guest interactions in these systems at atomic level we systematically study the effect of various factors in the process and unravel its key determinants. Density functional theory calculations have been employed. Our findings have the potential to be employed as guidelines in designing new HDAC inhibitors with improved anticancer properties.

Keywords: Cancer; Density Functional Theory; Histone Deacetylase Inhibitors; Molecular Modeling; SAHA;

Introduction

Cancer is a disease, driven by different, yet not fully understood mechanisms. Various genetic and genomic alterations (amplifications, translocations, deletions or point mutations) are considered to be the major underlying cause for tumor onset in mammals. However, there is a growing evidence that other mechanisms, involving epigenetic changes, are also in play in neoplastic tissue formation. Generally, these are related to aberrant DNA methylation and/or posttranslational histone modifications (acetylation, methylation or phosphorylation). Particularly, the disruptions in post-translational modifications (PTM) of chromatin structure promote uncontrollable cell growth branded as a hallmark of tumor lesions [1]. One of the PTM is the process of acetylation of histones. This is a reversible process, regulated by two groups of enzymes with antagonistic functions – histone deacetylases (HDACs) and histone acetyltransferases (HATs). HATs catalyze acetylation of histones, which, by reducing their positive charge and, subsequently, attenuating the strength of interactions with the DNA, results in relaxing the chromatin structure and promoting gene expression. On the other hand, HDACs are responsible for the deacetylation of histones, leading to stiffening/compacting of chromatin structure, which, in turn, causes transcriptional silencing [2]. Deregulation of HATs and HDACs activities has fatal consequences for the host organism: increased (abnormal) levels of HDACs and suppressed expression of HATs have been observed in several types of cancer tissues, suggesting that the overexpression/hyperactivity and aberrant recruitment of HDACs to their promoter region could be a common feature for the tumorogenesis and cancer progression [3]. Among the family of HDACs, the zinc-containing HDAC8, which plays a key role in a number of malignancies, such as T-cell lymphoma [4], childhood neuroblastoma [5], gastric cancer [6], colon cancer [7], breast cancer [8], and acute myeloid leukemia [9], is a promising therapeutic target for drug formulations that inhibit its enzymatic activity.

Based on their chemical structure, the HDAC inhibitors (HDACI) of HDAC8 are classified into several chemical classes: hydroxamic acids, benzamides, short chain fatty acids and cyclic tetrapeptides [10]. The hydroxamic acid – based HDACIs have analogous block structure, dictated by the specific geometry of the enzyme and its active site, comprising four pharmacophoric subunits: cap group, connecting unit, hydrocarbon linker and zinc-binding moiety [11,12]. These are shown in Figure 1 along with the structure of the most popular drug of this class - suberoylanilide hydroxamic acid (SAHA).

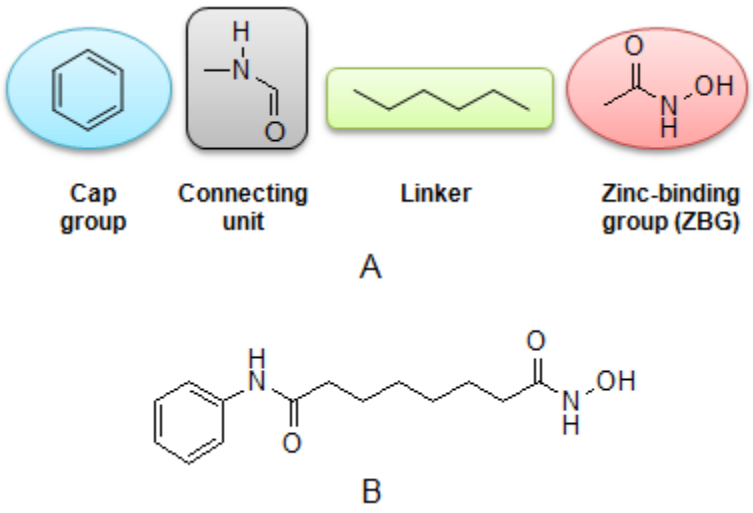

Figure 1. (A) Pharmacophoric model of HDACI and (B) structure of suberoylanilide hydroxamic acid (SAHA).

Each of the building blocks interacts specifically with a different region of the HDAC enzyme and has its own function. The cap group is usually aromatic and hydrophobic [13] and interacts with the outer layer of the active site [12,14]. The connecting (anilide) unit forms hydrogen bond contacts with amino acid the active site pocket. The linker is a saturated or unsaturated hydrocarbon chain with, in most cases, linear structure. It interacts with the hydrophobic tunnel (channel) leading to the enzyme active center. Zinc-binding group (ZBG), chelates the zinc ion in the active site. Properties of the ZBG correlate strongly with the potency of the HDAC inhibitor [15]. Chemical variations in the subunits generate drugs with different potency, selectivity and toxicity profiles.

HDAC8 binding site comprises an 11 Å – long channel (tunnel) and 14 Å – wide internal cavity [12]. The tunnel's entrance is rigid and its walls are hydrophobic. It leads to a buried internal cavity where the active site resides. Central to the catalytic activity of the enzyme is a Zn^{2+} ion, located in the active site. It is pentacoordinated in the HDAC8-SAHA complex (PDB entry 4QA0). Three coordination positions of the metal are occupied by two monodentate aspartate residues (Asp178 and Asp 267) and one histidine residue (His 180) donated by the host enzyme. Additionally, upon SAHA binding, zinc cation is ligated by the hydroxamate group from the inhibitor orbiting the metal in bidentate fashion (see Figure 2 below).

Although potent HDAC inhibitors such as trichostatin A [16], SAHA (Figure 1 and Scheme 1) [17] and MS275 [18] have been identified and characterized, they lack enough HDAC8 selectivity warranting further explorations for finding more selective HDACIs. Furthermore, the factors governing the process of HDAC8 – HDACI recognition are not very well understood and several outstanding questions regarding the intimate mechanism of the process are still waiting to be answered:

1. Which are the "key" (first-order) and "incremental" (second-order) interactions between the hydroxamic acid inhibitors and HDAC8 enzyme, and what is the contribution of different inhibitor building blocks to the magnitude of these encounters?
2. How do the affinity and selectivity of the inhibitor towards the HDAC8 enzyme changes with varying the length of the hydrocarbon linker and chemical structure of the cap group and connecting unit?
3. How do internal (structure and properties of the inhibitor) and external (dielectric properties and amino acid composition of the enzyme binding site) factors influence the affinity of the inhibitors towards HDAC8 enzyme?
4. What is the most plausible pharmacophore model for SAHA and its analogs when interacting with the HDAC8 enzyme?

Herein, in an attempt to shed light on the mechanism of the HDAC8 – HDACI recognition at atomic level and its physico-chemical descriptors, we systematically study the effect of various factors on the host-guest interactions and unravel key parameters governing the process. The interactions between the HDAC8 binding site (realistically modeled) and a series of 15 hydroxamic acid derivatives with variable chemical structure and properties (see Methods) are studied by employing density functional theory (DFT) calculations in conjunction with polarizable continuum model (PCM) computations. The influence of different factors on the thermodynamics of the host-guest interactions, such as the length of the hydrocarbon linker of the inhibitor, chemical structure of its connecting unit and cap group, properties of the metal's first and second-shell amino acid ligands, and dielectric characteristics of the enzyme binding pocket, are assessed. Note that our aim is to evaluate reliable trends of changes in the enzyme – inhibitor interaction energies rather than to reproduce their absolute values. The approach adopted has proven quite successful in evaluating the thermodynamic parameters of host-guest recognition in a number of biological systems such as enzymes [19], signaling proteins [20] and ion channels [21].

Methods

Inhibitor molecules

A number of hydroxamic acid derivatives were explicitly modeled and their interactions with the host HDAC8 active center were evaluated. The popular and well-studied HDAC inhibitor - SAHA is considered as a reference in this study and, therefore, its structure was taken as a template for various chemical modifications. The molecules considered are presented in Scheme 1.

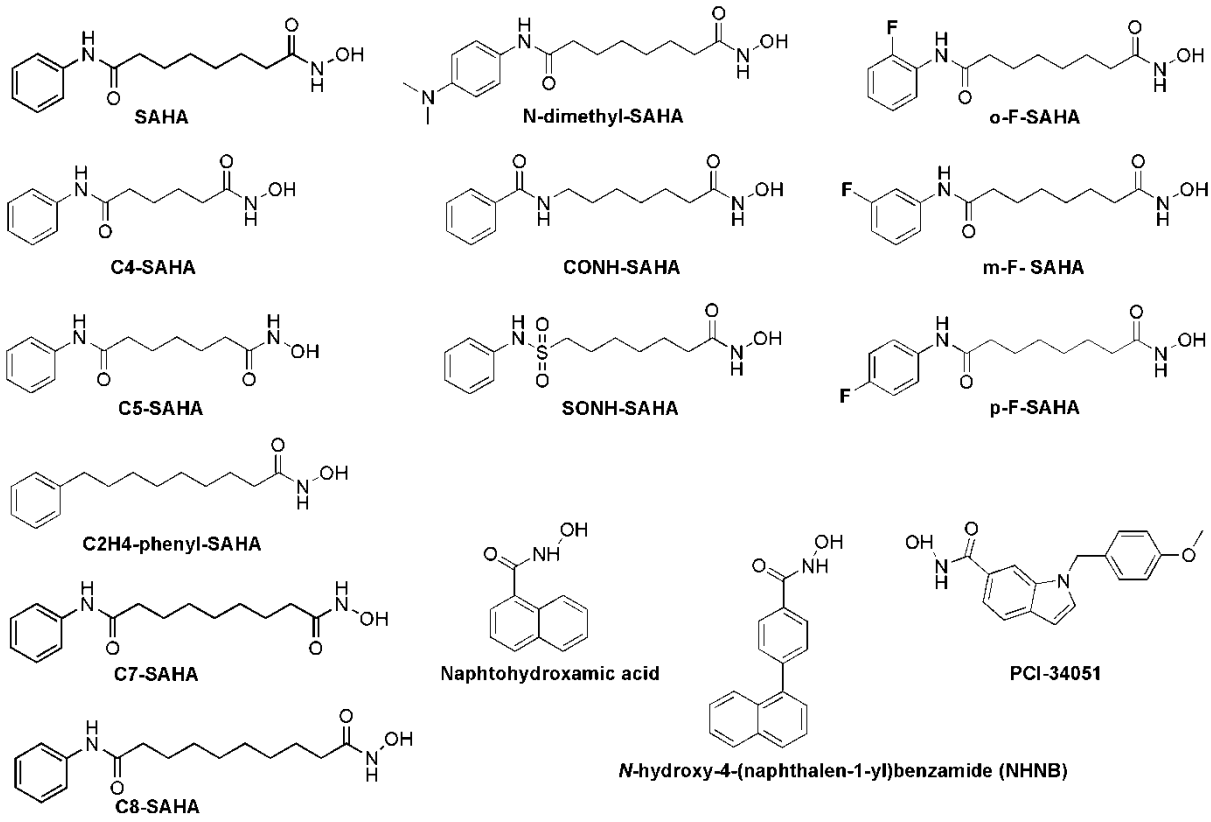

Scheme 1. Structure of the studied HDAC inhibitors

The series includes SAHA itself (comprising a 6-methylene group linker) and several of its analogs possessing the same cap group/connecting unit but different-length linkers, namely C4-SAHA (4-methylene-group linker), C5-SAHA (linker consisting of 5 methylene groups), C7-SAHA and C8-SAHA with 7 and 8 methylene-group linkers, respectively. Another subgroup incorporates SAHA derivatives comprising a linker with the same length (6 methylene groups) but having chemical alterations in the cap group: N-dimethyl-SAHA (benzene ring with para-substituted electron-donating N-dimethyl group) and three mono-fluorinated derivatives where the electron-withdrawing fluorine substituent occupies the respective ortho- (o-F-SAHA), meta- (m-F-SAHA) and para-positions (p-F-SAHA) in the benzene ring. A different subgroup includes SAHA derivatives with modified anilide moiety ("connecting unit"): CONH-SAHA, SONH-SAHA and C2H4-phenyl-SAHA (Scheme 1). Three linkerless hydroxamic-acid-based inhibitors of therapeutic value (Naphtohydroxamic acid, PCI-34051 and N-hydroxy-4-(naphthalene-1-yl)benzamide) [11] are also considered although their overall structure differs from that of SAHA.

HDAC8 active site modeling

The X-ray crystal structure of HDAC8 complexed with SAHA (pdb code: 4QA0, resolution of 2,242 Å) was used in modeling the enzyme active site with the bound inhibitor. In the process, the B chain of the enzyme was deleted and only the A chain and co-crystallized inhibitor were retained. Furthermore, using Raswin [22] and GaussView 06 [23] we deleted the amino acid residues, which are more than 3 Å away from SAHA in the active site. Zinc-coordinating residues (Asp178, Asp267 and His180) were retained. Tyr306, His142 and His143, which are implicated in contributing to the energetics of the host-guest complexation [12] were retained as well. Hydrogen atoms were added to all the amino acid residues. Each amino acid fragment was capped by a -CH_3 group at its C_α position. The structure of the model binding site used as a starting point for the subsequent calculations, is shown in Figure 2. SAHA was replaced at the same locality by its analogs in creating the respective HDAC8-inhibitor complexes.

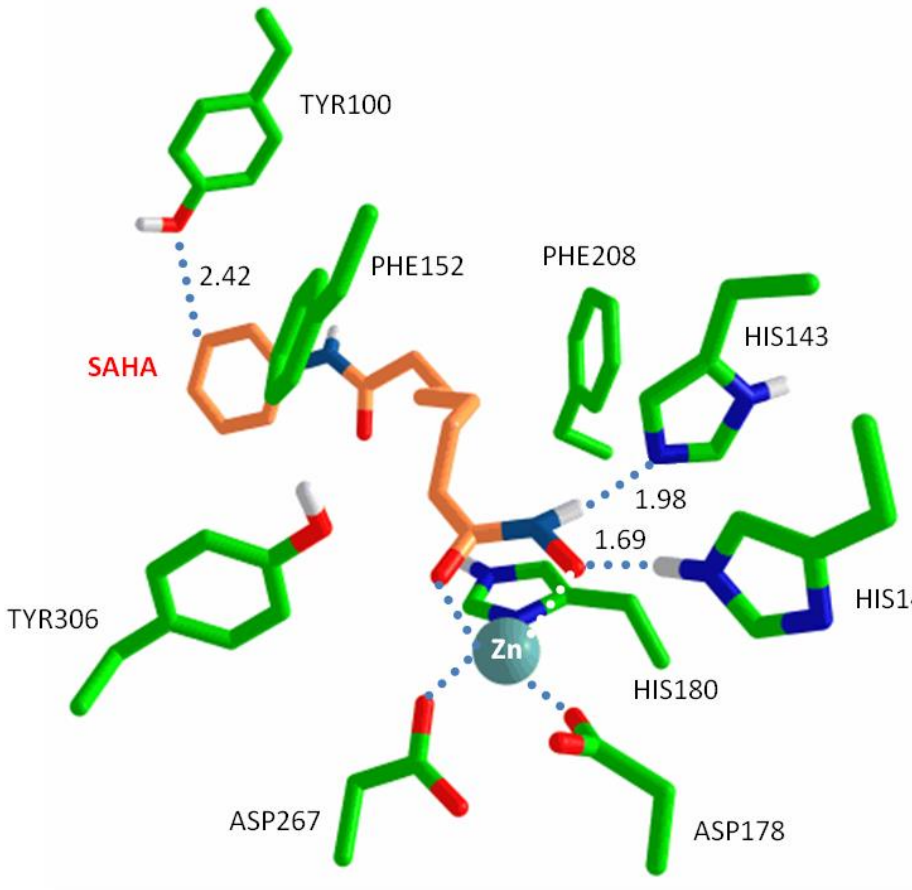

Figure 2. Active site of HDAC8 in complex with SAHA (Cut from PDB 4QA0).

DFT/PCM calculations

All calculations were performed employing Gaussian 09 program package [24]. The complexes between HDAC8 active site and inhibitors were optimized in the gas phase at B3LYP/6-31+G(d) level of theory yielding the respective electronic energies, E_{el}[1], of the studied constructs. This combination of method and basis set was chosen based on previous theoretical studies of hydroxamic acids [25] which demonstrated that this combination correctly describes the geometries and properties of these molecules and their derivatives, and also on

our own validation of the applicability of this combination through comparison with available experimental data (Table 1).

Table 1. Comparison between computed and experimental mean metal−oxygen and metal–nitrogen bond distances (in Å) in Zn^{2+}complexes

Complex	Bond	Experiment	B3LYP/6-31+G(d)
$[Zn(H_2O)_6]^{2+}$	Zn − O	2.08±0.03[a]	2.13
$[Zn(H_2O)_n(imidazole)_1]^{2+}$	Zn − N	2.00±0.02[b]	$[Zn(H2O)_5(imidazole)_1]^{2+}$: 2.03 $[Zn(H2O)_4(imidazole)_1]^{2+}$: 1.98 Average: 2.00

[a] From Ref [26] [b] Mean Zn–N bond distance based on data for 20 tetra- and pentacoordinate Zn –imidazole complexes in the Cambridge Structural Database; from Ref [27].

In order to preserve the integrity of the model binding site, the C_α position of each amino acid was kept frozen to its initial geometry during the optimization. All other geometrical parameters were let to relax. The solvation effects were accounted for by employing polarizable continuum model (PCM) calculations in water ($\varepsilon = 78$; fully solvent exposed surfaces) and methanol ($\varepsilon \approx 32$; mimicking less solvent accessible binding sites). The optimized structure of each molecule/complex in the gas phase was subjected to single point calculations in water and methanol. The difference between the gas-phase and PCM energies was used to calculate the solvation energy, $\Delta E_{solv}^{\varepsilon}$, of the respective entity: $\Delta E_{solv}^{\varepsilon} \approx E_{el}^{\varepsilon} - E_{el}^{1}$.

The affinity of the hydroxamic acids, listed in Scheme 1, toward HDAC8 has been studied. It can be expressed in comparative manner in terms of the energy change of the reaction, ΔE^x, for replacing SAHA bound to the active center of HDAC8 by its rival inhibitor (Eq. 1).

$$[Inh] + [SAHA\text{-}HDAC8] \rightarrow [Inh\text{-}HDAC8] + [SAHA] \quad (1)$$

In eq. 1, [Inh] and [SAHA] denote the free unbound inhibitors, whereas [SAHA-HDAC8] and [Inh-HDAC8] refer to the SAHA and rival inhibitor-loaded HDAC8, respectively. The reaction was modeled in the gas phase, methanol ($\varepsilon \approx 32$) and water ($\varepsilon = 78$). The gas-phase energy of SAHA→Inh substitution is given by

$$\Delta E^1 = E_{el}^1(Inh\text{-}HDAC8) + E_{el}^1(SAHA) - E_{el}^1(SAHA\text{-}HDAC8) - E_{el}^1(Inh) \quad (2)$$

whereas that in condensed phase, by

$$\Delta E^{\varepsilon} = \Delta E^1 + \Delta E_{solv}^{\varepsilon}(products) - \Delta E_{solv}^{\varepsilon}(reagents) \quad (3)$$

Positive ΔE^x implies a lower-affinity than SAHA inhibitor, while a negative value signifies the opposite.

Results and discussion

The effect of linker length

SAHA molecule coordinates to several entities from the HDAC8 active site (Figure 2) which, through electrostatic and van der Walls interactions, contribute to the stability of the complex: (a) the Zn^{2+} cation to whom it binds in a bidentate fashion via its hydroxamic head;

(b) hydrophobic Phe152 and Phe208 residues which surround its hexamethylene linker; (c) Tyr100 and Tyr306 which interact with its end anilide group. Additionally, upon optimization, the C=O group from the anilide fragment creates hydrogen bond with the H-N group from His180.

Would be there any changes in the inhibitor affinity and structure of its complex with HDAC8 upon altering the length of its linker chain? To answer this question we modeled complexes of the enzyme active site with several SAHA analogs possessing linkers comprising 4, 5, 7 and 8 methylene groups. The energies of replacing SAHA with its inhibitor counterparts in different dielectric media are presented in Table 2.

Table 2. Energies (in kcal/mol) of replacing SAHA with analogs containing variable length of linker chain in different dielectric media

Inhibitor	ΔE^{1}	ΔE^{78}	ΔE^{32}
SAHA	0	0	0
C4-SAHA	-0.24	0.34	0.36
C5-SAHA	-11.28	-8.61	-8.90
C7-SAHA	2.79	1.80	1.89
C8-SAHA	5.58	6.18	6.27

The results obtained imply that an inhibitor with 4-methylene-group linker has almost the same affinity toward the enzyme relative to its SAHA counterpart as the energies of SAHA→C4-SAHA substitution are insignificantly small. Increasing the length of the linker beyond that of SAHA (to 7 and 8 methylene groups) decreases the affinity of the inhibitor evidenced by positive values of ΔE throughout the entire dielectric range (Table 2). The longer the chain, the lower the affinity (higher ΔE for C8-SAHA than C7-SAHA). This is mainly due to attenuating the strength of the C=O(inhibitor)…H-N(His180) hydrogen bond in the series SAHA→C7-SAHA→C8-SAHA whose length increases from 1.96 Å to 2.01 and 6.70 Å, respectively. On the other hand, C5-SAHA appears to be more efficient than SAHA in binding the host enzyme as ΔEs of SAHA→C5-SAHA exchange stay firmly on a negative ground. Detailed analysis of the structure of C5-SAHA - HDAC8 complex (Figure 3) revealed that this is due to an additional stabilizing interaction between C5-SAHA and amino acid residue from the active center: The lack of one methylene group (as compared to SAHA) puts the anilide group from the linker unit of the inhibitor in an appropriate position for a hydrogen bond contact between the metal-free oxygen atom from the carboxylate group of Asp267 residue and the hydrogen atom from the NHCO group of C5-SAHA (Figure 3). Note that the hydrogen bond between C=O(inhibitor) and H-N(His180) characteristic for SAHA (see above) is weakened, although not severed (bond distance of 2.20 A), and stronger N-H(inhibitor) … -OOC(Asp267) hydrogen bond is created instead (bond length of 1.95 Å)

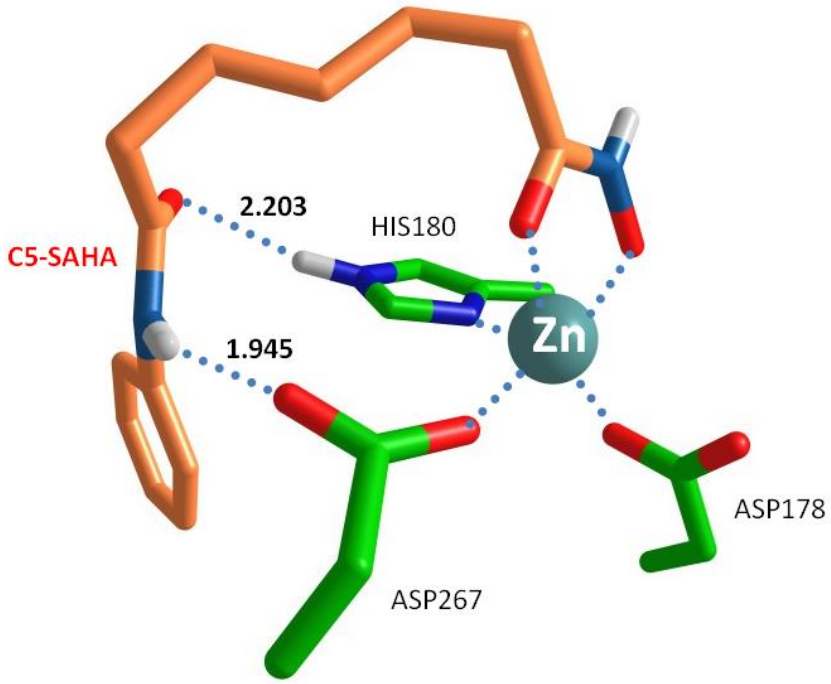

Figure 3. “Key” interactions between C5-SAHA and HDAC8 active site.

Note that the degree of solvent exposure of the active site does not significantly influence the thermodynamics of the SAHA→inhibitor exchange (similar ΔEs for each reaction in the last two columns of Table 2).

Furthermore, the alterations in the inhibitor linker length do not affect the structure (and consequently the energetics) of the metal center of the enzyme, as its geometrical parameters deviate within very narrow limits throughout the series (Table 3). Thus, differences in the relative affinity of the inhibitors toward the host enzyme could be largely attributed to the specific characteristics of their linker, connecting unit and cap moieties.

Table 3. Calculated distances (in Å) between Zn^{2+} and its ligands in the HDAC8 active site.

Inhibitor	NH (hydroxamic head)	O=C (hydroxamic head)	Asp267	His180	Asp178
SAHA	2.14	2.13	2.06	2.15	2.01
C4-SAHA	2.14	2.16	2.03	2.15	2.02
C5-SAHA	2.13	2.12	2.10	2.15	2.00

C7-SAHA	2.16	2.11	2.05	2.15	2.02
C8-SAHA	2.14	2.13	2.05	2.16	2.02

The effect of modification of the cap moiety

The energies of replacing SAHA from the enzyme active site by its analogs comprising the same hexamethylene linker but with chemically altered benzene ring from the cap group are presented in Table 4.

The substitution of SAHA with benzene-substituted analogs is thermodynamically favourable and characterized with a small decrease in reaction energy. Neither the electronic nature of the substituents nor their position in the benzene ring seem to play a role in the energetics of the process as both the N-dimethyl (electron-donating substituent) and fluorine (electron-accepting substituent) derivatives yield similar energies of the SAHA→inhibitor exchange encompassing few kcal/mol in condensed media. Structural analysis of the inhibitor complexes reveals an additional, though not very strong, interaction (which is missing in the cognate SAHA) between a phenyl C-H bond and the metal-free oxygen atom from Asp267 (bond distance between 2.1 and 2.4 A; figure not shown).

Table 4. Energies (in kcal/mol) of replacing SAHA with analogs containing substituted benzene ring in different dielectric media

Inhibitor	ΔE^{1}	ΔE^{78}	ΔE^{32}
SAHA	0	0	0
N-dimethyl-SAHA	-0.94	-1.20	-1.19
o-F-SAHA	-5.13	-1.78	-1.86
m-F-SAHA	-0.92	-0.22	-0.25
p-F-SAHA	-4.94	-1.08	-1.39

Again, as in the previous series of inhibitors (see above), alterations in the remote part of the hydroxamic acid do not affect the structure and energetics of the metal center of the enzyme.

Modifications in the connecting anilide NHCO group

Next examples reveal the importance of the NHCO anilide group for the energetics of the inhibitor - HDAC8 recognition: C2H4-phenyl-SAHA, devoid of such a group, cannot compete successfully with SAHA for the enzyme as it lacks additional stabilizing interactions (as discussed above for SAHA) with amino acid residues from the binding pocket (evidenced by positive ΔEs of SAHA→C2H4-phenyl-SAHA exchange in Table 5).
Along the same vein, replacing the anilide NHCO group with an amide one, CONH, yields a lower-affinity CONH-SAHA inhibitor (relative to SAHA) as it, due to steric reasons, misses the hydrogen bond contact between the C=O(inhibitor) and N-H(His180) groups (Figure 4). On the other hand, strong intramolecular hydrogen bonds between sulfonamide group and partner amino acids render the SAHA→SONH-SAHA reaction favorable in condensed media (negative ΔE^{78} and ΔE^{32} in Table 5).

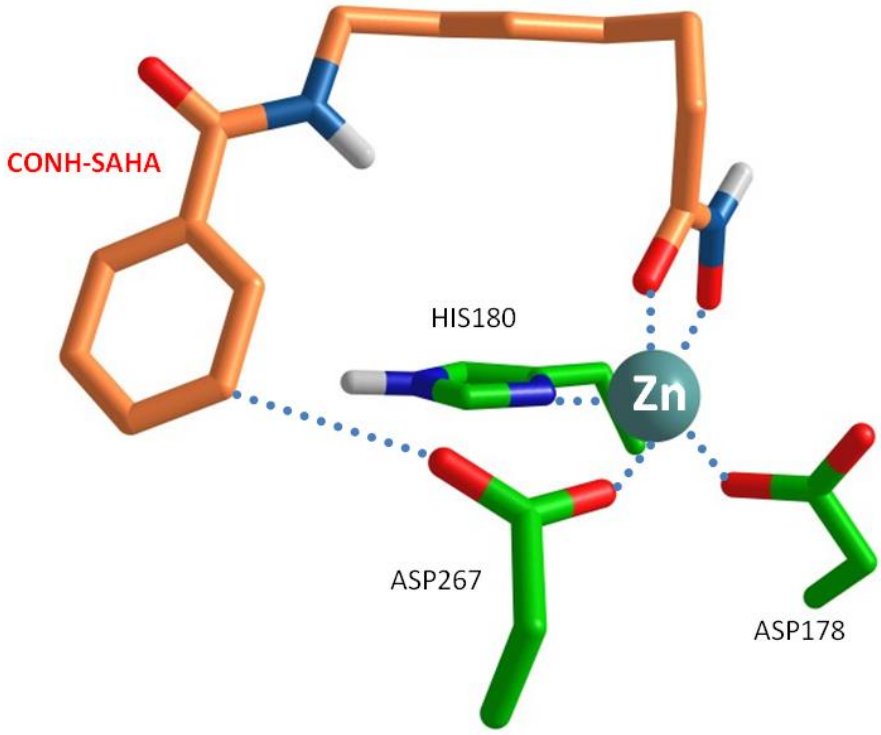

Figure 4. Lack of hydrogen bond contact between the C=O(inhibitor) and N-H(His180) groups between CONH-SAHA and HDAC8 active site.

Table 5. Energies (in kcal/mol) of replacing SAHA with analogs containing modified connecting anilide group in different dielectric media

Inhibitor	ΔE^{1}	ΔE^{78}	ΔE^{32}
SAHA	0	0	0
C2H4-phenyl-SAHA	1.63	2.48	2.52
CONH-SAHA	-0.97	3.06	2.88

SONH-SAHA	0.36	-1.03	-1.01

Linkerless inhibitors

Table 6 lists energies for the competition between SAHA and three linkerless inhibitors. Not surprisingly, all the energies are positive suggesting lower relative affinities for these molecules. This is mostly due to the specific structure of these inhibitors which is devoid of hydrocarbon linker and anilide group thus missing important stabilizing interactions with the host enzyme, as discussed above. Furthermore, the relatively bulky aromatic groups attached immediately to the hydroxamic head of the inhibitor do not fit nicely to the narrow channel leading the active center of the enzyme.

Table 6. Energies (in kcal/mol) of replacing SAHA with linkerless inhibitors in different dielectric media

Inhibitor	ΔE^{1}	ΔE^{78}	ΔE^{32}
SAHA	0	0	0
Naphtoxydroxamic acid	2.85	4.47	4.71
PCI34051	6.23	5.78	5.95
N-hydroxy-4-(naphthalen-1-yl)benzamide (NHNB)	1.65	0.32	0.33

Conclusion

Complexes between HDAC8 binding site and a series of hydroxamic acid inhibitors were modeled and their energies relative to that of the cognate SAHA were evaluated. Through analyzing the key and incremental interactions within the inhibitor – enzyme complexes the specific factors governing the affinity and selectivity of the inhibitor for the host enzyme have been identified.

The calculation revealed two **"key interactions**" in the enzyme-inhibitor system which determine the affinity towards the HDAC8 enzyme: (1) the interaction between the oxygen atom from the anilide group of SAHA or the sulfonamide group of its analogs, and hydrogen atom from His180. The absence of such interaction in other representatives of the series (e.g. C2H4-phenyl-SAHA and C8-SAHA) relegates the inhibitor to the lower-affinity zone. (2) the interaction between hydrogen atom from anilide group of the inhibitor and carboxylate oxygen from Asp267 residue from the active site of the enzyme. It was found that this interaction is the strongest in the C5-SAHA-HDAC8 complex. It is obvious, that the availability of this interaction directly correlates with the significantly greater affinity of C5-SAHA, towards HDAC8 than all other hydroxamic acids, where this interaction is absent. The role of the "connecting unit" (anilide, amide or sulfonamide group) in determining the inhibitor affinity and selectivity toward the host enzyme should be emphasized. Thus, our findings suggest reclassification of this moiety as a different structural unit of its own right, along with the

hydroxamic head, hydrocarbon linker and aromatic cap units, in the pharmacophore model of SAHA and the like inhibitors.

There are lower-energy ("**incremental**") interactions which also stabilize, though in lesser extent, the enzyme-inhibitor system: interactions between the carboxylate oxygen from Asp267 from the enzyme active site and hydrogen atoms from the benzene ring in the cap unit (see for example the benzene-substituted SAHA derivatives above). Although, these interactions are significantly weaker than the "key interactions" mentioned above, it is highly likely that they also have a contribution for the affinity of hydroxamic acids towards the HDAC8 enzyme.

Among the amino acid residues, surrounding the metal in the active site, Asp267 and His180 appear to play a key role not only in binding the Zn^{2+} cation, but in shaping the affinity and selectivity of the inhibitor molecule. Other amino acid residues in this locality, such as Asp178, His142 and His143, were found not to participate in key or incremental interactions with the guest molecule thus not contributing to the process of HDAC8-inhibitor recognition.

Furthermore, analyzing the bond lengths between the zinc cation and hydroxamic moiety in different enzyme-inhibitor complexes, it was found that the geometry (and, respectively, the energetics) of the metal center does not alter upon changes in the linker, connecting unit and cap moieties of SAHA analogs. Thus, the affinity and selectivity of hydroxamic acid derivatives relative to those of the cognate SAHA molecule are shaped mainly by the structural and physicochemical characteristics of those fragments. A hydroxamic acid derivatives comprising hexa- or pentamethylene linker, sulfonamide "connecting unit" and substituted aromatic ring seem to be highly efficient HDAC8 inhibitors for the antitumor therapy.

Conflict of Interests

There are no conflicts to declare

Acknowledgements

The authors are thankful for the support by Sofia University Science Fund, contract № 80-10-21/18.03.2020

References

[1] Haberland, M.; Montgomery, R. L.; Olson, E. N. *Nat. Rev. Genet.* **2009**, *10*, 32-42.
[2] Struhl, K. *Genes dev*. **1998**, *12*, 599-606.
[3] Ropero, S.; Esteller, M. *Mol. Oncol.* **2007**, *1*, 19-25.
[4] Oki, Y.; Younes, A.; Copeland, A.; Hagemeister, F.; Fayad, L. E.; McLaughlin, P.; Shah, J.; Fowler, N.; Romaguera, J.; Kwak, L. W.; Pro, B. *Br J Haematol.* **2013**, *162*, 138-141.
[5] Oehme, I.; Deubzer, H. E.; Wegener, D.; Pickert, D.; Linke, J.-P.; Hero, B.; Kopp-Schneider, A.; Westermann, F.; Ulrich, S. M.; von Deimling, A.; Fischer, M.; Witt, O. *Clin Cancer Res.* **2009**, *15*, 91-99.
[6] Song, S.; Wang, Y.; Xu, P.; Yang, R.; Ma, Z.; Liang, S.; Zhang, G. *Int J Oncol.* **2015**, *47*, 1819-1828.
[7] Nakagawa, M.; Oda, Y.; Eguchi, T.; Aishima, S.-I. ; Yao, T.; Hosoi, F.; Basaki, Y.; Ono, M.; Kuwano, M.; Tanaka, M.; Tsuneyoshi, M. *Oncol. Rep.* **2007**, *18*, 769-774.

[8] Hsieh, C.-L.; Ma, H.-P.; Su, C.-M.; Chang, Y.-J.; Hung, W.-Y.; Ho, Y.-S.; Huang, W.-J.; Lin, R.-K. *Life Sci*. **2016**, *151*, 7-14.
[9] Kirschbaum, M. H.; Foon, K. A.; Frankel, P.; Ruel, C.; Pulone, B.; Tuscano, J. M.; Newman, E. M. *Leuk. Lymphoma*, **2014**, *55*, 2301-2304.
[10] Dokmanovic, M.; Marks, P. A. *J. Cell. Biochem.* **2005**, *96*, 293-304.
[11] Tabackman, A. A.; Frankson, R.; Marsan, E. S.; Perry, K.; Cole, K. E. *J. Struct. Biol*. **2016**, *195*, 373-378.
[12] Bourguet, E.; Ozdarska, K.; Moroy, G.; Jeanblanc, J.; Naassila, M. *J. Med. Chem.* **2018**, *61*, 1745-1766.
[13] Somoza, J. R.; Skene, R. J.; Katz, B. A.; Mol, C.; Ho, J. D.; Jennings, A. J.; Luong, C.; Arvai, A.; Buggy, J. J.; Chi, E.; Tang, J.; Sang, B. C.; Verner, E.; Wynands, R.; Leahy, E. M.; Dougan, D. R.; Snell, G.; Navre, M.; Knuth, M. W.; Swanson, R. V.; McRee, D. E.; Tari, L. W. *Structure*, **2004**, *12*, 1325-1334.
[14] Choi, S. E.; Pflum, M. K. H. *Bioorg. Med. Chem. Lett.* **2012**, *22*, 7084-7086.
[15] a) Cheshmedzhieva, D.; Toshev, N.; Gerova, M.; Petrov, O.; Dudev, *J. Mol. Model.* **2018** *24*, 114; b) Cheshmedzhieva, D.; Toshev, N.; Gerova, M.; Petrov, O.; Dudev, T. *Bulg. Chem. Commun*. **2018,** *50(J)* 228-236.
[16] Yoshida, M.; Kijima, M.; Akita, M.; Beppu, T. *J. Biol. Chem.* **1990**, *265*, 17174-17179.
[17] Duvic, M.; Vu, J. *Expert Opin. Investig. Drugs.* **2007**, *16*, 1111-1120.
[18] Bracker, T. U.; Sommer, A.; Fichtner, I.; Faus, H.; Haendler, B.; Hess-Stumpp, H. *Int. J. Oncol.* **2009**, *35*, 909-920.
[19] Dudev, T.; Cheshmedzhieva, D.; Doudeva, L. *J. Mol. Model.* **2018**, *24*, 55.
[20] Dudev, T.; Grauffel, C.; Lim, C. *Inorg. Chem.* **2018**, *57*, 14798-14809.
[21] Dudev, T.; Lim, C. *Acc. Chem. Rev.* **2014**, *47*, 3580-3587.
[22] Sayle, R. A.; Milner-White, E. J. RASMOL: biomolecular graphics for all. *Trends Biochem Sci.* **1995**, *20*, 374-376.
[23] GaussView, Version 5, Roy Dennington, Todd Keith and John Millam, Semichem Inc. Shawnee Mission KS. 2009.
[24] Gaussian 09, Revision A.02, M. J. Frisch, G. W. Trucks, H. B. Schlegel, G. E. Scuseria, M. A. Robb, J. R. Cheeseman, G. Scalmani, V. Barone, B. Mennucci, G. A. Petersson, H. Nakatsuji, M. Caricato, X. Li, H. P. Hratchian, A. F. Izmaylov, J. Bloino, G. Zheng, J. L. Sonnenberg, M. Hada, M. Ehara, K. Toyota, R. Fukuda, J. Hasegawa, M. Ishida, T. Nakajima, Y. Honda, O. Kitao, H. Nakai, T. Vreven, J. A. Montgomery, Jr., J. E. Peralta, F. Ogliaro, M. Bearpark, J. J. Heyd, E. Brothers, K. N. Kudin, V. N. Staroverov, R. Kobayashi, J. Normand, K. Raghavachari, A. Rendell, J. C. Burant, S. S. Iyengar, J. Tomasi, M. Cossi, N. Rega, J. M. Millam, M. Klene, J. E. Knox, J. B. Cross, V. Bakken, C. Adamo, J. Jaramillo, R. Gomperts, R. E. Stratmann, O. Yazyev, A. J. Austin, R. Cammi, C. Pomelli, J. W. Ochterski, R. L. Martin, K. Morokuma, V. G. Zakrzewski, G. A. Voth, P. Salvador, J. J. Dannenberg, S. Dapprich, A. D. Daniels, . Farkas, J. B. Foresman, J. V. Ortiz, J. Cioslowski, D. J. Fox, Gaussian, Inc., Wallingford CT, **2009**.
[25] a) Yang, J.; Bremer, P. J.; Lamont, I. L.; McQuillan, A. J. *Langmuir*, **2006**, *22*, 24, 10109–10117; b) Przychodzeń, W.; Chojnacki, J. *Struct. Chem.* **2008*, 19,*** 637–644.
[26] Dudev, T.; Lim, C. *J. Am. Chem. Soc.* **2006**, *128*, 1553– 1561.
[27] Harding, M. M. *Acta Cryst.* **1999**, *D55*, 1432–1443.